Journal of Catalysis 258 (2008) 334–344

Contents lists available at ScienceDirect

Journal of Catalysis

www.elsevier.com/locate/jcat

Correlations between synthesis, precursor, and catalyst structure and activity of a large set of $CuO/ZnO/Al_2O_3$ catalysts for methanol synthesis

C. Baltes, S. Vukojević, F. Schüth *

Max-Planck-Institut für Kohlenforschung, Kaiser-Wilhelm-Platz 1, 45470 Mülheim an der Ruhr, Germany

ARTICLE INFO

Article history:
Received 25 February 2008
Revised 30 June 2008
Accepted 3 July 2008
Available online 3 August 2008

Keywords:
Copper
Zinc
Aluminum
Catalyst
Coprecipitation
High throughput experimentation
Methanol synthesis
Syngas
Reaction conditions
TPR

ABSTRACT

Ternary $Cu/ZnO/Al_2O_3$ catalysts were systematically prepared via the coprecipitation route under strict control of parameters such as pH, precipitation temperature, and calcination temperature. All catalysts were tested with respect to their methanol synthesis activity in a 49-fold multitubular high-throughput experimentation setup under conditions similar to the commercial methanol production route, using a syngas mixture of CO, CO_2, and H_2. Representative samples were chosen for a more detailed structure and morphology analysis to reveal correlations between the catalyst's "preparation history" and the methanol productivity. The best catalytic performance was observed for catalysts obtained from precursors precipitated in the pH range of 6–8 at 70 °C. XRD measurements allowed the "grouping" of catalysts based on their phases. It was found that a group of best-performing catalysts exhibited the characteristic XRD pattern of nondecomposed Cu/Zn hydroxy carbonate residues in the calcined precursors, leading to the assumption that carbonate species in this state may enhance productivity. Further investigations of these hydroxy carbonate-containing catalysts provided more detailed insight into the dynamic aging process and its affect on catalytic performance. The greatest methanol synthesis activity was observed for catalysts aged for 20–60 min after an initial phase formation time. The optimum calcination temperature was found to be in 250–300 °C. Under these conditions, the resulting Cu/Zn/Al hydroxy carbonates remained stable. In addition, the syngas feed composition was varied under reaction conditions and correlated to catalytic activities. The greatest methanol productivity over $Cu/ZnO/Al_2O_3$ catalysts was observed for the following gas concentrations: 50–60% for H_2, 30–40% for CO, and 5–10% for CO_2, at 4.5 MPa and 245 °C.

1. Introduction

$Cu/ZnO/Al_2O_3$ catalysts are used predominantly in the industrial low-pressure methanol synthesis process starting from synthesis gas, a mixture of H_2, CO, and CO_2. To date, the best catalytic performance has been achieved over $Cu/ZnO/Al_2O_3$ catalysts prepared by the coprecipitation method using nitrates of Cu, Zn, and Al and alkali bicarbonates or alkali carbonates as basic precipitating agents. The resulting hydroxy carbonates are converted to metal oxides by subsequent calcination at ca. 300–500 °C. The final active catalyst is obtained by reduction of CuO to metallic Cu under a diluted H_2 flow before feeding the synthesis gas mixture [1–3]. Each step in the synthetic procedure may influence the activity of the final catalyst under reaction conditions, the structure of which may be different from that of a sample recovered after the reaction and analyzed ex situ. Numerous studies have evaluated sample sets covering a limited part of the parameter space or parts of the full catalyst synthesis sequence. Several of these studies focused on the binary Cu/ZnO system. Due to the somewhat fragmented data in the literature, it seemed worthwhile to undertake a more comprehensive study of the whole sequence from hydroxy carbonate precursor over oxide precursor to the reduced catalyst in the $Cu/ZnO/Al_2O_3$ system, and to attempt to elucidate the influence of the conditions and the structure of the solid after each step on the final activity of the catalyst.

The role of metallic copper in the reaction mechanism has been widely discussed in the literature over the past 20 years and remains a matter of debate. Today, it is widely accepted that metallic copper clusters are the active sites for the methanol synthesis reaction over Cu/ZnO-based catalysts [4,5]. The main function attributed to the ZnO is to increase Cu dispersion in the calcined sample, thus providing a high number of active sites exposed to the reaction gases [1]. In addition, however, ZnO may contribute to the high activity through some other effects, as discussed below.

Studies on the phases in the precipitate of Cu/Zn hydroxy carbonates in combination with aging effects have revealed that some precipitate phases seem to favor the dispersion of copper. For instance, in aurichalcite $(Cu,Zn)_5(CO_3)_2(OH)_6$, Cu is atomically dispersed in a zinc hydroxy carbonate matrix, whereas in zincian-

* Corresponding author. Fax: +49 208 306 2995.
E-mail address: schueth@mpi-muelheim.mpg.de (F. Schüth).

0021-9517/$ – see front matter
doi:10.1016/j.jcat.2008.07.004

malachite $(Cu,Zn)_2(OH)_2CO_3$, Cu is atomically substituted by Zn in the typical malachite structure. Subsequent calcination leads to the formation of small CuO crystallites believed to be the ideal intermediates for obtaining the final reduced catalyst. In addition, dissolution of small amounts of Cu^{2+} ions in the ZnO framework has been suggested to contribute to the high degree of copper dispersion [6]. The addition of M^{3+} ions (e.g., Al^{3+}) has been reported to increase the BET surface area and copper dispersion while inhibiting the sintering of Cu particles under on-stream conditions [7,8]. The nature and arrangement of carbonate residues in the calcined ternary $Cu/ZnO/Al_2O_3$ catalyst structure and their contribution to catalyst performance has not been studied in detail to date.

Schlögl et al. [9] investigated another possible function of the ZnO in the catalyst (or rather in the hydroxy carbonate precursor). They found that for Cu/ZnO catalysts derived from hydroxy carbonates (the industrial catalyst synthetic route), the copper lattice is strained compared with bulk copper, and that this strain correlates with high methanol synthesis activity [9]. Therefore, strained copper particles, brought about by the close interaction with the ZnO, may have a greater intrinsic activity for methanol synthesis than bulk-structured copper.

As mentioned above, the classical hydroxy carbonate route leads to the formation of several mixed-metal hydroxy carbonates, including aurichalcite $[(Cu,Zn)_5(CO_3)_2(OH)_6]$, zincian-malachite $[(Cu,Zn)_2(OH)_2CO_3]$, and a Cu–Zn hydrotalcite-like phase $[(Cu,Zn)_6Al_2(OH)_{16}CO_3{\cdot}4H_2O]$. All of these phases decompose to give well-dispersed oxidic phases [10,11]. It is known from studies on Cu/ZnO hydroxy carbonate systems that the presence of residual carbonate in the calcined sample plays an important role, supposedly due to subsequent formation of a copper suboxide species, increasing the chemical activity of catalysts [12]. One motivation for the ongoing research into the chemical and structural nature of these precursors is the presumed conjunction with the activity of the final catalyst. The final catalyst is created in a multistep procedure, with each preparation step contributing separately to the catalyst properties. So far, few comparative studies on the effects of various synthesis procedures on the catalyst activity exist. These studies often lack detailed information on reaction parameters and reveal contradictory findings [8,13,14]. Most studies of coprecipitated systems have dealt with the zinc–copper catalyst, assuming that effective investigation of the industrial catalyst system can be done successfully only with a firm knowledge of the binary system.

Over the past 10 years, high-throughput experimentation (HTE) has proven to be a reliable technology for the evaluation and development of solid catalysts [15–17]. Methanol synthesis is an interesting example reaction for applying high-throughput techniques, because it is a very time-consuming reaction due to the need for high-pressure conditions for satisfactorily high conversions and the carefully conducted catalyst activation and reduction processes. Taking into account the industrial reduction and reactor startup period, even superficial catalyst testing by conventional means may take several days. Our HTE parallel reaction setup allows us to operate as closely as possible to single-channel conventional catalyst testing while saving time through an initial *collective* catalyst pretreatment [18]. The conditions applied during the activation and reaction periods are very close to the industrial standard.

The objective of the present study was to systematically investigate the synthesis/structure/activity relationships of the ternary Cu/Zn/Al methanol synthesis catalyst at different steps in catalyst preparation by high-throughput methods. The main focus is the study of different preparation parameters during the precursor formation process and their influence on methanol productivity. Numerous catalysts were tested for their methanol synthesis activity by high-throughput screening, and interesting samples were analyzed in more-detailed studies. In particular, selected catalysts and precursor materials were investigated with regard to phase and morphology changes induced by aging effects and calcination procedures.

2. Experimental

2.1. Catalyst preparation

Ternary $CuO/ZnO/Al_2O_3$ catalysts were prepared by coprecipitation analogous to the coprecipitation procedure described by Kiener et al. [18]. A solution of metal nitrates [($Cu(NO_3)_2$ (0.6 mol/L), $Zn(NO_3)_2$ (0.3 mol/L), $Al(NO_3)_3$ (0.1 mol/L))] and a solution of Na_2CO_3 (1 mol/L) as a precipitant were pumped (at constant flow rate of 5 ml/min) into a stirred and heated glass reactor with a starting volume of 200 ml of demineralized water. During the precipitation process, pH, temperature and aging time were controlled. While the metal nitrate solution was being pumped continuously, the sodium carbonate solution was added to maintain a constant pH (±0.1 unit), controlled by a WTW 296 pH meter. The coprecipitation was stopped when 40 mL of metal nitrate solution had been added. The pH was kept constant also during the aging process through the controlled addition of metal nitrate or sodium carbonate solution except in the studies of the aging process, where some batches were aged without pH control ("free aging"). After aging for 1 h, the precipitates were filtered and washed three times with 150 mL of demineralized water each, and then dried overnight at 80 °C. After grinding, 200–500 mg of the dried hydroxy carbonate precursor was calcined at 300 °C under air for 3 h (heating ramp 2 °C/min), resulting in the oxide precursor.

2.2. Characterization

Transmission electron microscopy (TEM) was done with a Hitachi HF 2000 operated at 200 kV, equipped with a cold-field emission gun at a beam energy of 200 kV and NORAN Instruments Si (Li) EDX spectrometer for point resolved elemental analysis. Solid samples were dry-prepared on lacey carbon-coated nickel grids.

The metal contents of the precursors and catalysts were determined by energy-dispersive X-ray (EDX) analysis, performed on a Hitachi S-3500N scanning electron microscope equipped with an Oxford EDX system.

X-ray diffraction (XRD) measurements were performed on a STOE STADI P transmission X-ray powder diffractometer equipped with a linear position sensitive detector using $CuK\alpha_1$ radiation. XRD patterns were recorded in the range of 5–80° (2θ).

Temperature-programmed reduction (TPR) was performed in a special flow reactor, using a gas mixture of 5 vol% H_2 in nitrogen at a flow of 90 ml/min. The reactor was heated up to 300 °C at a ramp rate of 6 °C/min. Typically, 50 mg of catalyst powder was used as a sample. Before measurement, the sample was heated in nitrogen atmosphere to 120 °C (10 °C/min). To study the Cu amount of the catalysts, the time-resolved H_2 consumption peak was integrated. For determination of copper content via this method, reduction from CuO to Cu was assumed.

Nitrogen adsorption was done using a NOVA Quantachrome 3200e Multi-Station High-Speed Gas Sorption Analyzer, version 7.30. Before analysis, samples were activated under vacuum at 150 °C for 2 h. Isotherms were recorded at 77.3 K. N_2-physisorption was used to characterize the surface area. The BET surface area was calculated from the adsorption data in the relative pressure interval from 0.04 to 0.2.

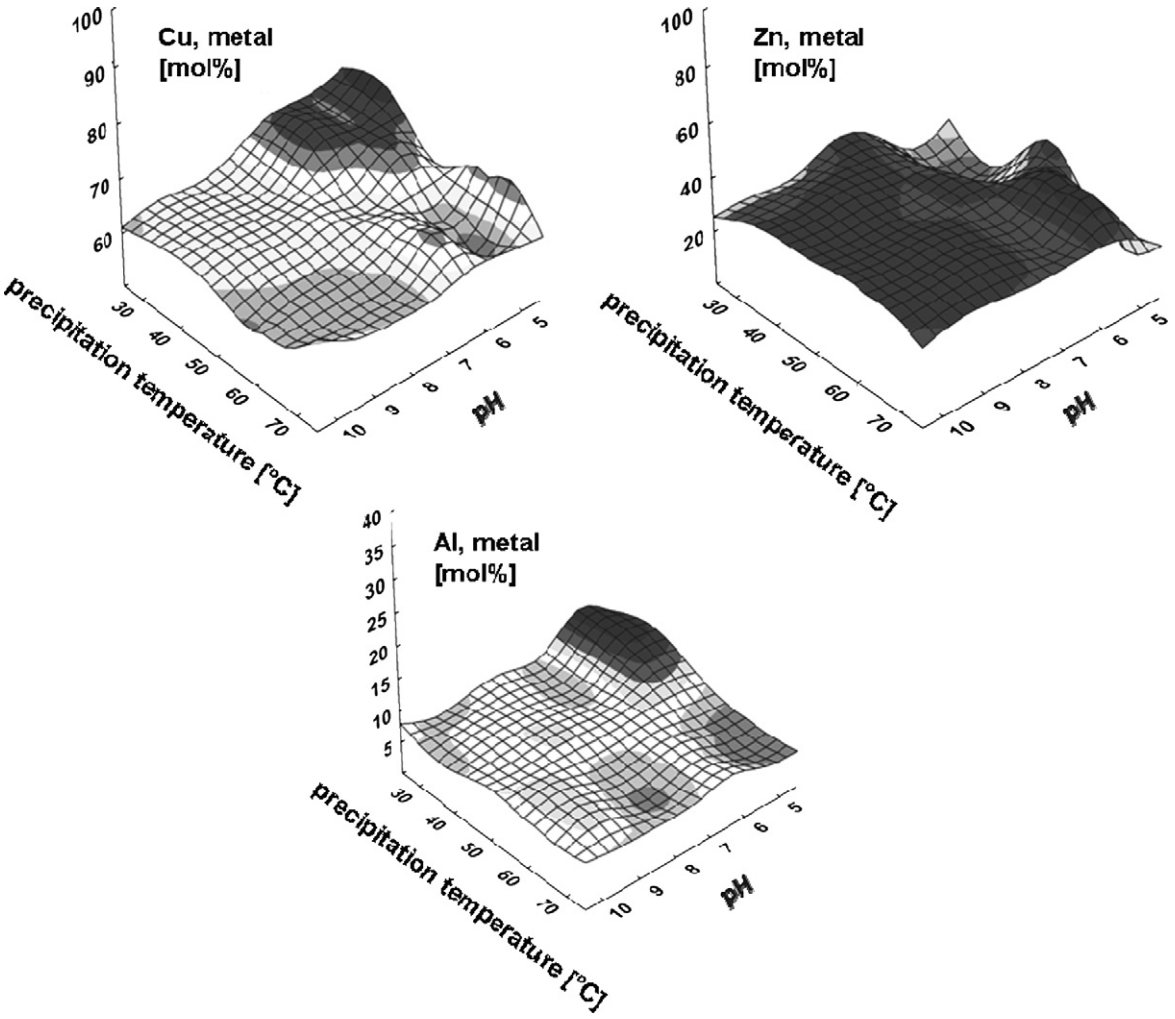

Fig. 1. Influence of the precipitation conditions on the catalyst metal content (excluding oxygen).

A parallel reactor setup in combination with a spatially resolving FTIR FPA system in rapid scan mode has been developed that can simultaneously analyze the specific surface area of 15 copper catalysts, as described in detail elsewhere [19]. The system allows the reliable determination of copper surface areas with an error of about ± 1 m^2/g.

2.3. Catalytic measurements

Catalytic measurements were performed in a high-throughput 49-channel parallel reactor described elsewhere [18]. The oxide precursor samples (ca. 50 mg as received sample, diluted with 200 mg of quartz sand per channel) were placed in a sample holder consisting of a stainless steel cartridge closed at the bottom with a stainless-steel sinter metal frit. Before the catalytic measurements, the precursors were reduced with a 5% H_2/N_2 mixture at 245 °C following the procedure for the commercial benchmark catalyst ICI Katalco 51–8. Before the catalytic activity measurements, all samples were equilibrated for 3 h (reaction pressure 4.5 MPa, reaction temperature 245 °C, analytic flow 20 ml/min). For the standard conditions, the reaction gas consisted of 70 vol% H_2, 24 vol% CO, and 6 vol% CO_2. A double-GC system (HP GC 6890) was used for online gas analysis. A full analysis of low-molecular-mass carbon compounds was completed within 6 min. The methanol productivity of all of the measured samples was compared with that of the industrial benchmark catalyst ICI Katalco 51-8 ($P_{ICI} = 40$ mol MeOH/(kg_{cat} h) at 245 °C and 4.5 MPa).

3. Results and discussion

Initially, two identical sets of hydroxy carbonate precursors (each containing 35 catalysts) were prepared by the coprecipitation method at pH 4.5–10 and precipitation temperature of 30–70 °C. All precursors underwent controlled aging for 1 h in the mother liquor and were calcined under air atmosphere for 4 h at 300 °C. A 50-mg sample of each precursor was used for the activity screening.

3.1. Elemental analysis

A total of 25 catalysts and precursors from the first set of catalysts, representing samples over the entire range of precipitation parameters, were investigated by EDX analysis. The Cu/Zn/Al metal ratio in the precipitated hydroxy carbonate as well as in the calcined precursors corresponded to the metal ratio, which was set by the precursor solution concentrations. The ratio appeared to be independent of the preparation conditions. Within a range of ± 5 mol%, the Cu/Zn/Al metal ratio was found to be 60/30/10 mol%. These results are in very good agreement with the intended metal composition, which had been selected with regard to the commonly used commercial catalyst. Fig. 1 shows the hydroxy carbonate precursor metal content depending on the precipitation conditions. As described above, the Cu/Zn/Al ratio was found to be almost constant over the entire parameter range. Only at relatively low precipitation temperatures (30 °C) and acidic conditions

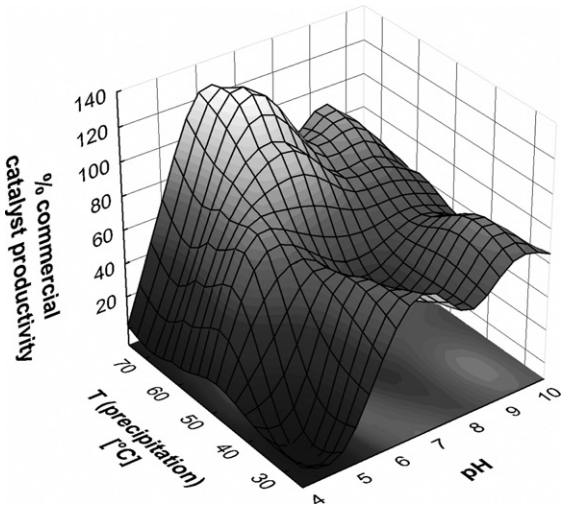

Fig. 2. Influence of the catalyst preparation conditions (pH and precipitation temperature) on methanol productivity measured at 245 °C and 4.5 MPa. Productivity of the commercial catalyst under these conditions: 40 mol MeOH/(kg_{cat} h).

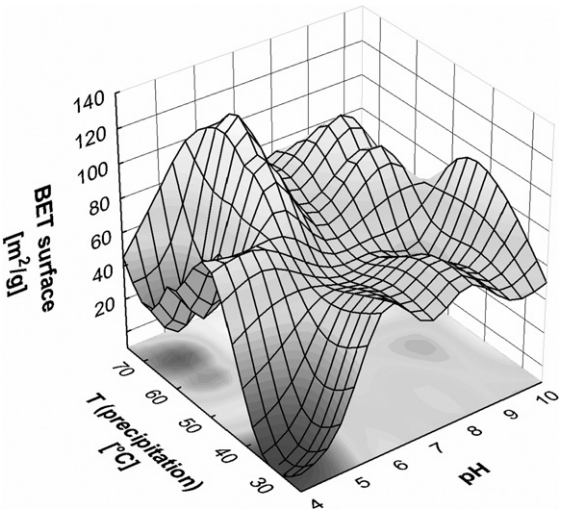

Fig. 3. Influence of the catalyst preparation conditions (pH and precipitation temperature) on the catalyst BET surface areas.

(pH 5) were increases in Cu content up to 72 mol% and Al content up to 12 mol% observed. Consequently, a lower Zn concentration (16 mol%) was found under these conditions.

In general, most of the catalysts investigated consisted of 40–50 wt% Cu, 20–25 wt% Zn, 3–5 wt% Al, and 25–30 wt% O. Furthermore, the amount of Cu corresponded closely with the CuO amount of 60 ± 5 wt% (i.e., 45 wt% Cu), found by TPR analysis for some selected samples (see below).

3.2. Catalytic screening

The catalyst productivities of nominally identical catalysts of the two sets differed by 5–10% at most, indicating that the overall process from precursor precipitation over calcination, reduction, and catalytic test could be reproduced at an acceptable level. The preparation–productivity relationship is shown in Fig. 2. The catalytic performance depended strongly on the precipitation conditions. The best productivities (exceeding those of the commercial catalyst by as much as 30%) were obtained at neutral or even slightly acidic pH (i.e., pH 6–7). The materials with the best catalytic performance were obtained by precipitation at about 70 °C; however, these catalysts also exhibited the strongest deactivation during time on stream, with activity level decreasing to the same level as that of the commercial benchmark over the course of several hours. The reasons for this deactivation of the high-activity catalysts are currently under investigation.

Generally, precipitation at temperatures above 50 °C led to a strong increase in the catalysts' methanol productivity. Surprisingly, the productivity rose rapidly when pH was increased only slightly from 4.5 to 5; this occurred especially at relatively high precipitation temperatures. The optimum conditions found here correspond to those often cited in the literature [20–22], although many studies have used significantly different conditions.

3.3. BET and specific copper(0) surface area

BET surface areas were determined for the set of catalysts used for the activity screening. Fig. 3 shows the correlation of the catalyst surface area and the preparation conditions. In general, surface areas in the range of 2–110 m^2/g were found. Comparing Fig. 3 with the preparation/activity plot in Fig. 2 shows good agreement between some parts of both plots. At slightly acidic conditions (pH 4–5) and low precipitation temperatures, catalyst surface areas of a few square meters per gram corresponded well to the

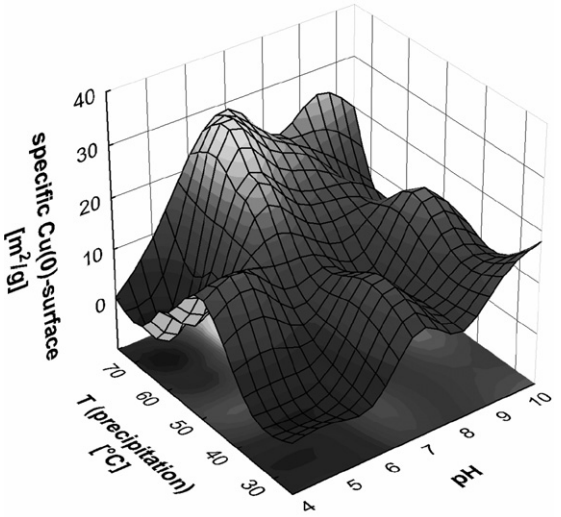

Fig. 4. Influence of the catalyst preparation conditions (pH and precipitation temperature) on the catalyst Cu(0) surface areas.

low MeOH productivity of the catalysts. Furthermore, the best-performing catalysts found at 70 °C and pH 6–8 (100–130% of the benchmark catalyst activity) also had relatively high surface areas (90–110 m^2/g). For the catalysts obtained at high precipitation temperatures, a significant increase of BET surface areas was seen. Li and Inui [20] used identical recipes as for some of the catalysts from the parameter field investigated here; they found that overall, the surface areas were lower by about a factor of 2, but the trend of increasing surface area with increasing pH and increasing precipitation temperature held.

Copper(0) surface areas were determined for the aforementioned catalyst set. Surface areas in the range of 28 to <1 m^2/g were found. Fig. 4 shows the correlation between the specific Cu(0) surface and the preparation conditions. Catalysts with low Cu(0) surface areas (0.5–2 m^2/g) were seen in the low-pH region (pH 4–5) at temperatures of 30–40 °C. With increasing pH values and precipitation temperatures, an increase in Cu(0) surface areas (up to 10 m^2/g) was seen. Samples obtained at high precipitation temperatures (>60 °C) and acidic conditions (pH <5) demonstrated decreasing Cu(0) surface areas (<5 m^2/g). Higher precipitation temperatures favored the formation of catalysts with relatively high Cu(0) surface areas. Generally, two parameter ranges

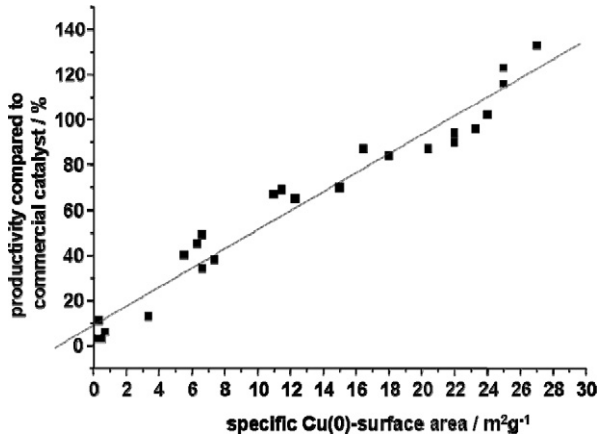

Fig. 5. Correlation of specific Cu(0) surfaces and catalyst performance of Cu/ZnO/Al_2O_3 catalysts.

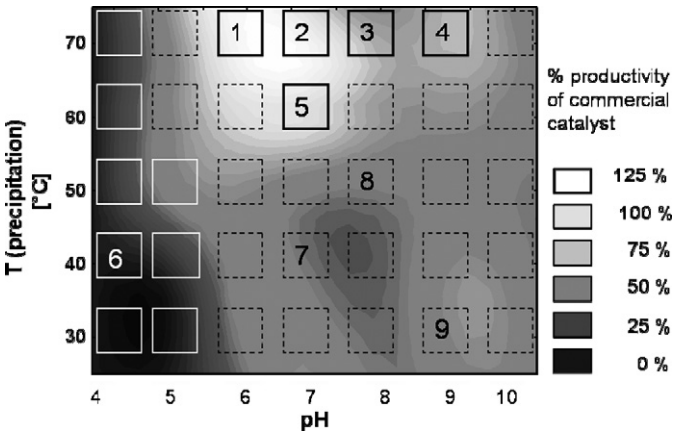

Fig. 6. Methanol productivity/preparation mapping of the tested catalyst set, clustering of catalysts based on their XRD signature: cluster 1 (full black line) including catalysts Cat_1–Cat_5, Cat_6 given as examples for cluster 2 (white line), cluster 3 (dashed black lines) represented by catalyst samples Cat_7–Cat_9.

were found for high Cu(0) surfaces: 24–28 m^2/g at pH 9–10 and $T > 65\,°C$ and 25–30 m^2/g at pH 6–7 and $T > 60\,°C$.

Fig. 5 shows a plot of catalyst productivity versus specific Cu(0) surface. In good agreement with previous studies [23–25], a linear correlation was found for all measured Cu/ZnO/Al_2O_3 catalysts. Note, however, that catalysts prepared by significantly different methods did not necessarily fall on this line [26]; thus it is clear that additional effects, such as the strain discussed by Schlögl et al. [9], were coming into play.

3.4. Characterization of calcined precursors

Precursors for all catalysts from the first set prepared were evaluated by XRD. For samples of interest, samples of the second set were analyzed under the same conditions to validate the results. No significant deviations for the two sets were observed.

Fig. 6 shows the two-dimensional preparation/activity plot, assigning square-shaped fields to the prepared and examined samples from the full range of preparation conditions. Generally, the oxide precursors can be grouped into three clusters with regard to their XRD signature. Representative samples from each cluster are coded with numbers. Fig. 7 shows their XRD patterns.

The XRD patterns of the precursors produced under acidic conditions (pH 4.5 and 5 at 30 and 40 °C) reveal defined reflections that can be assigned to large crystallites of CuO. In addition, characteristic reflections for ZnO can be seen. Al_2O_3 was not seen as a separate phase and may have been present as amorphous material.

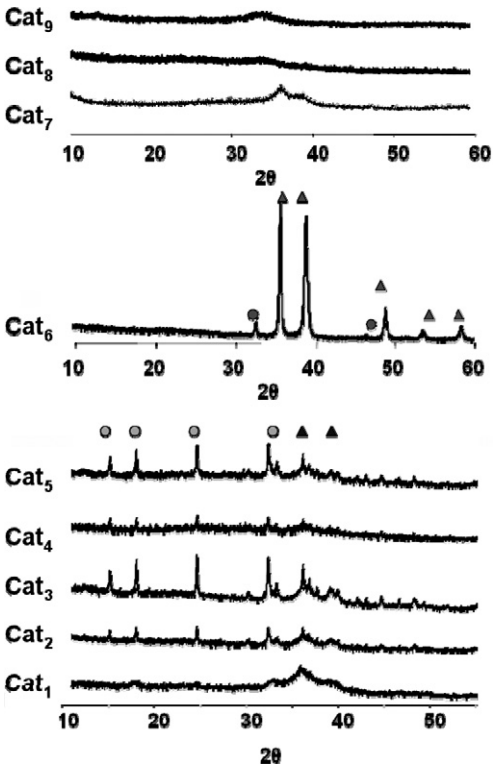

Fig. 7. XRD patterns of few selected calcined catalysts: (●) ZnO; (▲) CuO; (●) Cu/Zn-malachite, $(Cu,Zn)_2(OH)_2CO_3$.

These samples, marked as white-lined squares in Fig. 6, exhibited very low catalytic performance (0–5%) compared with the benchmark methanol catalyst. Cat_6 is a representative sample for this cluster of catalysts.

A second cluster comprises catalysts Cat_1–Cat_4, precipitated at 70 °C and at pH 6–9, and Cat_5, obtained at 60 °C and pH 7. All of the catalysts in this cluster are framed by solid black lines (cluster 1, Fig. 6). As shown in Fig. 7, calcined precursors from cluster 1 exhibited XRD patterns typical for copper or copper/zinc hydroxy carbonates. The phases identified were malachite and zincian-malachite [rosasite, $(Cu,Zn)_2(OH)_2CO_3$].

The main reflections and intensities corresponded to the pure and mixed malachite types. These hydroxy carbonate phases likely are residues originating from the precipitated precursor material, which was not completely decomposed during calcination. These findings correspond to literature reports describing rosasite and malachite as favored precipitation phases for an atomic Cu concentration >20 mol% [7]. The narrow peaks indicate that malachite was present as a well-defined crystalline phase.

As shown in Fig. 6, there is a clear correlation between the samples containing hydroxy carbonate residues after calcination (cluster 1) and the high methanol synthesis activity of the final catalyst. Most of the catalysts that reached 100% or more of the benchmark catalyst productivity contained nondecomposed residues of the malachite phase. The presence of this phase after calcination seemed to enhance the catalytic activity of the Cu/ZnO/Al_2O_3 mixed oxide material. Schlögl et al. identified high-temperature stable carbonates in their study of the binary Cu/Zn system over a wide range of compositions and related it to the presence of either aurichalcite or an unidentified phase [7]. In later work, they suggested that such high-temperature carbonates may be related to high catalytic activity after the analysis of binary Cu/ZnO catalysts, the precursors of which had been formed in a micromixer [27]. Such residual carbonates may be responsible for the formation of highly active sites. As reported by many authors,

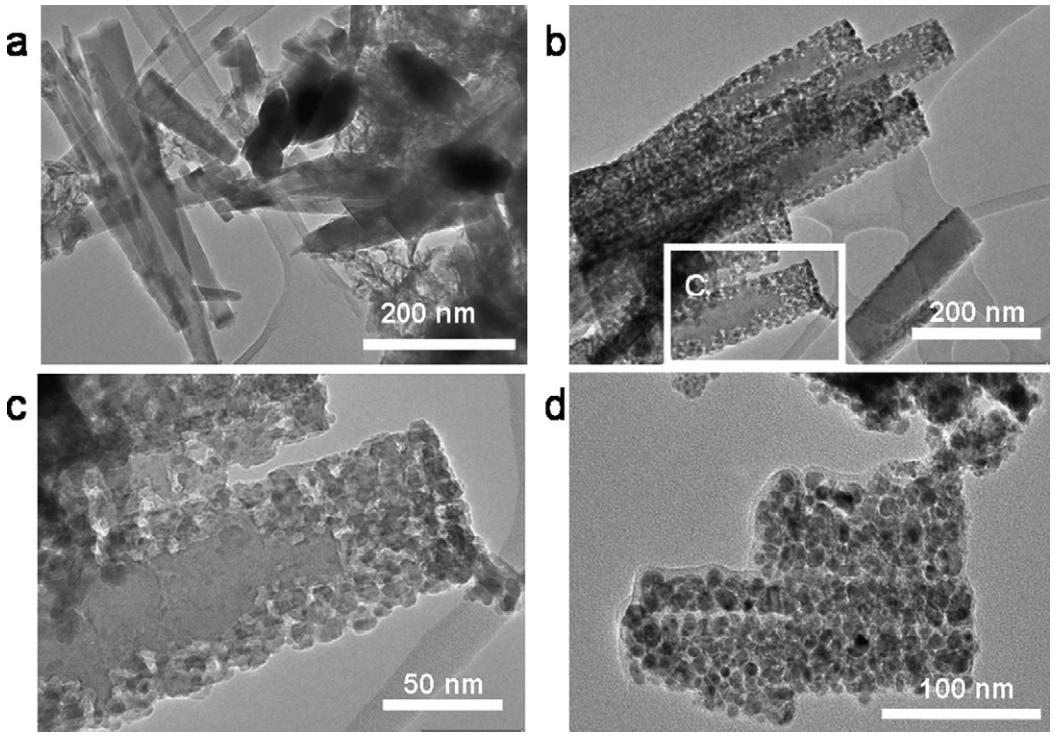

Fig. 8. TEM images of Cat_2: changes in catalyst morphology depending on the preparation steps: (a) catalyst precursor aged for 1 h, (b) catalyst calcined at 300 °C, (c) magnification of white framed area from image (b), (d) catalyst after reduction under H_2 atmosphere.

the calcination of mixed Cu/Zn hydroxy carbonate or hydrotalcite-like phases leads to the formation of smaller CuO and ZnO crystals compared with those derived from single phases, such as "pure" malachite. But the nature and arrangement of the CO_3^{2-} units remaining in the mixed oxide have not been examined in detail to date [28]. Nevertheless, most speculation about the productivity-enhancing properties of the carbonates present after calcination deals with the decomposition process; CO_2 released during the heating process in catalyst reduction may modify the reductive power of the gas phase and thus facilitate a "gentler" reduction process.

The calcined precursors of catalyst samples Cat_1–Cat_5 also exhibited the characteristic reflections for CuO in the XRD profiles. The reflections were very broad, indicating an ill-defined crystalline phase, probably overlapping with broad ZnO reflections. For samples obtained at other precipitation conditions, either broad reflections for CuO were seen in the XRD profiles or the samples were completely X-ray amorphous. Some representative XRD patterns for such systems (Cat_7, Cat_8, and Cat_9) are depicted in Fig. 7. The broad reflections and the low signal intensity strongly indicate that a substantial number of the samples precipitated at neutral and basic conditions at 30–60 °C were X-ray amorphous.

The TEM micrographs shown in Fig. 8 illustrate the changes in sample morphology occurring during the preparation procedure. Cat_2 (Fig. 6) was chosen for a more detailed study, because it exhibited the highest catalytic activity.

The hydroxy carbonate precursor aged for 1 h comprised mainly large clusters of needles, along with agglomerates of snowflake-shaped small crystals and platelets as minor components (Fig. 8a). This finding is consistent with the results of Whittle et al. [29], who studied the development of precursor morphology under aging conditions and found the formation of needle-like structures after aging for 1 h, starting from irregularly shaped grains.

EDX revealed that this needle phase and the platelets were copper-enriched and contained almost no aluminum (atomic ratio Cu/Zn = 4:1), whereas the flake-like phase exhibited a Cu/Zn/Al ratio of 3:2:1.

The needle-shaped crystallites underwent a morphological change during the calcination at 300 °C: Fig. 8b shows the formation of small particles (ca. 10 nm) at the edges of the needle-shaped crystallites, likely due to successive fragmentation of the precursor phase. The composition of the particles was analyzed by EDX measurements, resulting in a Cu/Zn ratio of 4:1. A tiny but constant amount of Al (2 at%) also was found. The area highlighted by a white frame in Fig. 8b is enlarged in Fig. 8c, providing a more detailed view of the particle–bulk interface. Needle-shaped particles also were found as products of a Cu/ZnO precursor produced in a micromixer [27]. In this study, very small ZnO (ca. 2 nm) clusters were detected in an amorphous matrix. This heterogeneity of the primary particles also may be a possible origin of the observed fragmentation of the needle-shaped crystals in our study, even if the system differs somewhat from that studied by Bems et al.

Fig. 8d provides some insight into the catalyst morphology after reduction under H_2 atmosphere, following the typical reduction procedure for the benchmark catalyst. The reduction was performed in a fixed-bed reactor, and the sample was then transferred under inert gas atmosphere to an argon-filled glovebox. The sample was placed onto a lacey carbon-coated Ni grid and transported in an air-protected transfer holder to the TEM instrument. The fragmentation observed for the reduced sample seems to be an ongoing process during reduction, explained by the thermal treatment of the sample (250 °C for 5 h), the reducing conditions, or combined effects.

From Fig. 8c, it is clear that fragmentation and the formation of particles had no effect on overall needle shape of the crystallites. Similar results were found for the reduced sample; however, the degree of fragmentation was higher than in other samples (Fig. 8d). The particle size did not change during the reduction procedure.

Results from EDX analysis of the sample revealed that the amount of oxygen was below that expected for oxidized Cu species. This suggests that the particles consisted mainly of re-

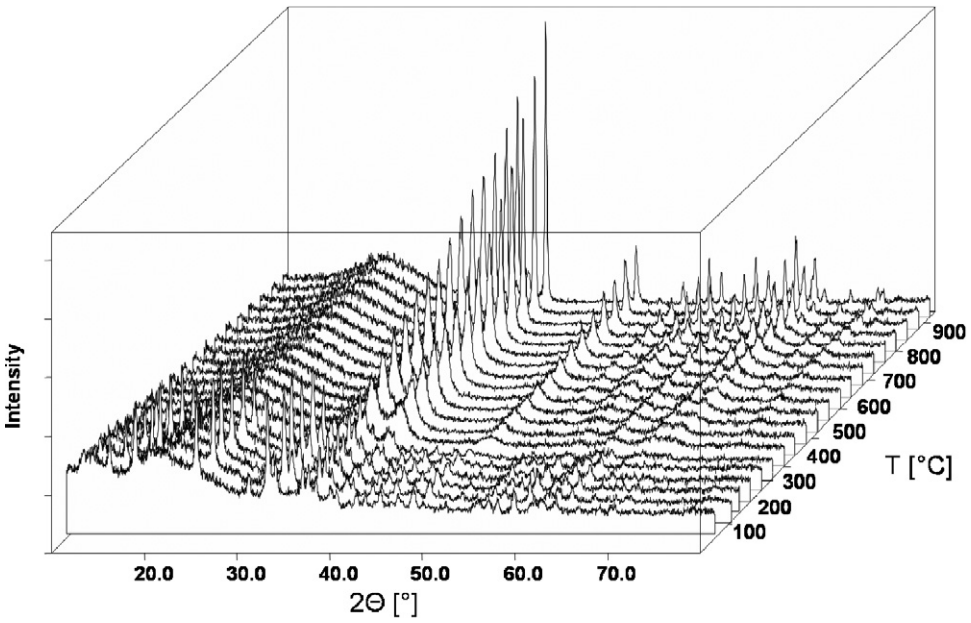

Fig. 9. *In situ* temperature-programmed XRD measurements of the Cat_2-precursor.

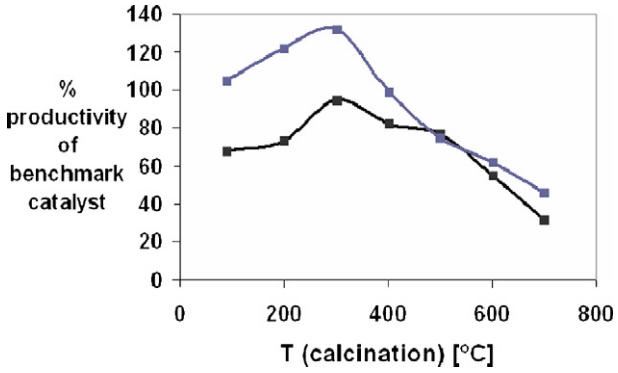

Fig. 10. Influence of the calcination temperature on the methanol productivity (black line and symbols) Cat_2, (grey line and symbols) Cat_4.

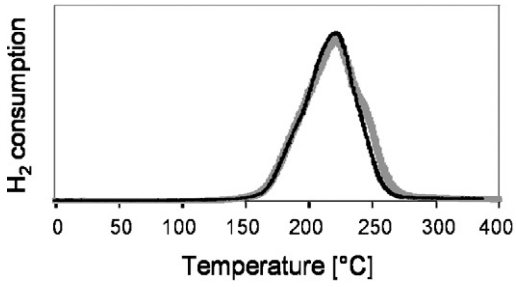

Fig. 11. TPR profile of Cat_2: (grey line) Cat_2 precursor, (black line) Cat_2 calcined.

duced or zero-valent Cu. The composition of particles did not change during the reduction treatment. The copper particles appear closely connected to the ZnO particles, creating a high degree of interfacial contact. This particle interaction dramatically enhanced the catalytic performance of the samples studied. These observations are in good agreement with results obtained by Ressler et al. [30], who also studied the strong Cu/Zn interaction and its correlation with the catalytic activity.

The role of nondecomposed hydroxy carbonate residues in the catalytic process was studied in more detail by performing a series of XRD measurements of the precursor for a highly active catalyst (Cat_2 in Fig. 6). The sample was heated stepwise in an *in situ* chamber from 100 to 900 °C, with the corresponding diffraction patterns recorded at each temperature level. The XRD patterns are plotted in Fig. 9. The influence of the calcination temperature on the methanol productivity is illustrated in Fig. 10. Two representative catalyst precursors, precipitated at 70 °C and pH 9 and 7, were calcined at 200, 300, 400, 500, 600, and 700 °C, and their catalytic activity was measured in the high-throughput setup. In addition, the noncalcined precursors were investigated for their methanol productivity, because TPR measurements revealed an almost complete overlap of the hydrogen consumption peak profiles (Fig. 11). Furthermore, no significant difference in reduction temperature was seen. Thus, it should be possible to carry out calcination of the hydroxy carbonates and reduction of copper(II) species in a single step.

TPR experiments were also used to study the reduction profiles of other selected samples. All of the highly active catalysts analyzed showed reduction peaks in a narrow range of 220–240 °C that were very similar for different samples. Samples precipitated under more acidic pH had higher reduction temperatures, in agreement with the larger CuO particles found in these samples by XRD. In addition to the particle size effect, the shift in reduction peaks also may be due to the presence of mixed oxides.

The amount of bulk copper was calculated from the reduction peaks. Assuming a reduction from CuO to Cu, a CuO content of 60 ± 5 wt% was found for most samples, in good agreement with the EDX data. But the reduction process may have been more complex, and only partially reduced copper species may have been left in the samples. Nonetheless, the agreement between the EDX and the TPR data with respect to the copper content demonstrates that these would be minority species.

For better comparability, Fig. 12 replots some of the XRD traces from Fig. 9 at characteristic temperatures. At the start of the temperature-programmed experiments, the precursor of Cat_2 had the diffraction pattern of Cu/Zn malachite, $(CuZn)_2(OH)_2CO_3$, with characteristic reflections at $2\theta = 15°$, 18°, 24°, 32°, and 36°. At 360 °C, the peak intensity decreased rapidly, and the malachite diffraction pattern began to disappear. Up to 380 °C, the hydroxy carbonate phase and the CuO phase coexisted. On further temperature increases, the characteristic CuO diffraction peaks at 35° and 39° increased in intensity. At 380–700 °C, ongoing growth of CuO

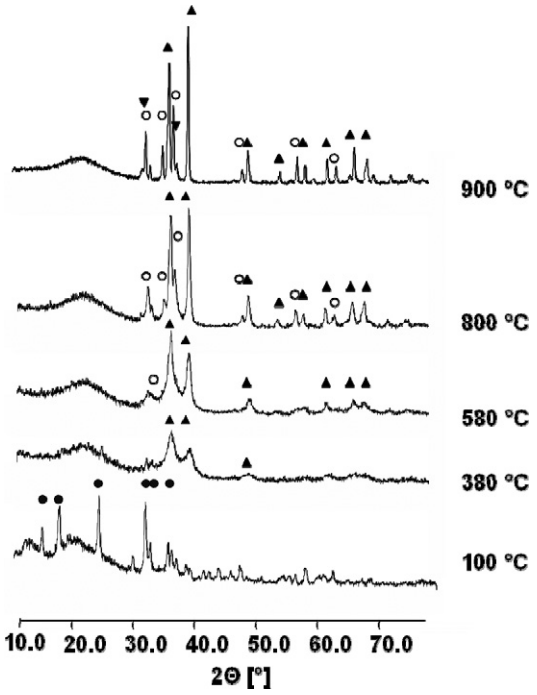

Fig. 12. Phase changes of Cat_2 as a function of calcination temperature monitored by *in situ* XRD measurement: (●) Cu/Zn malachite $(CuZn)_2(OH)_2CO_3$; (▲) CuO; (○) ZnO; (▼) $ZnAl_2O_4$ (gahnite).

particles was seen, indicated by the more pronounced and narrower reflections. At temperatures above 700 °C, reflections of pure ZnO became more prominent (reflections at 32°, 34°, and 36°). Finally, further heating of the sample to 900 °C resulted in a phase composition consisting of CuO, ZnO, and a tiny amount of $ZnAl_2O_4$ (gahnite).

Catalytic activity measurements of catalysts obtained by direct reduction of the dried precursor material following the standard reduction protocol yielded surprisingly high methanol productivity; for example, Cat_2 exhibited approximately 100% of the benchmark catalyst performance. As shown in Fig. 10, the methanol productivity initially increased with increasing calcination temperature, and then declined rapidly for calcination above 300 °C. An overly high calcination temperature is known to be detrimental to catalyst activity; a maximum temperature of 450–500 °C has been suggested [31]. We observed decreasing activity already at substantially lower temperatures of calcination for the samples shown in Fig. 10, and the differences in the activity profile between these and other samples demonstrates that the exact temperature differs for each preparation.

This finding may be viewed as providing further evidence of the productivity-enhancing effect of the hydroxy carbonate precursors. As reported above, all oxide precursors calcined at 300 °C that led to catalysts with high productivity contained residual hydroxy carbonate (Zn/Cu-malachite) phases (Fig. 6). The activity-enhancing effect associated with the presence of carbonate residues may originate from the partial decomposition during calcination. This effect may be compensated for at temperatures above 350 °C, probably due to the start of thermal sintering of the dispersed CuO particles.

3.5. Precursor state and aging effects

As reported previously, the postprecipitation aging time in the mother liquor can strongly influence the catalytic activity [32]. Consequently, the synthesis of selected catalysts from the activity study was reproduced, and the "preparation history" was recorded

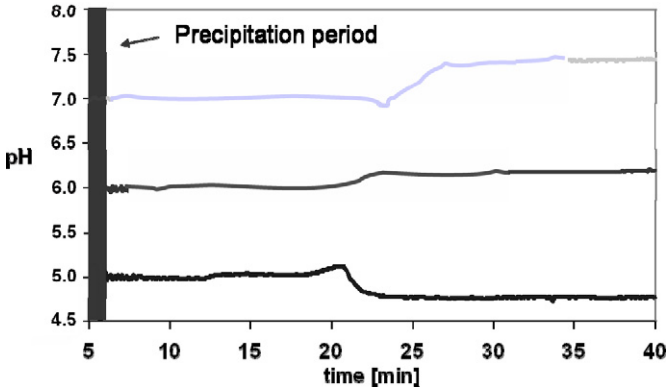

Fig. 13. pH evolution with time during free aging of three selected catalyst precursors obtained at pH 5, 6 and 7 (all at 70 °C).

in detail. Samples were obtained during the precipitation process while comparing the pH-controlled catalyst aging process and the so-called "free-aging" synthesis. For the free-aged precipitation, no additional metal nitrate or sodium carbonate solution was added to the suspended precipitate after the controlled precipitation period. The samples were investigated by XRD, and their methanol productivity was compared.

The free-aged precursor suspension was found to be a dynamic system, demonstrating time-dependent changes in the pH, as shown in Fig. 13 for some representative samples. All uncontrolled catalyst precursors seemed to undergo changes 20 and 40 min after completion of precipitation. Precursors obtained at lower pH exhibited a slight pH increase (0.1 units) after 10 min of free aging and subsequently reached a plateau, followed by a rapid drop in pH by 0.3–0.4 units. Precipitates produced at moderately acidic conditions showed a slight increase of pH (0.1 units) after 20 min, reaching a constant pH value thereafter. A more pronounced pH change was observed for precursors precipitated at neutral or slightly basic conditions; these exhibited a strong pH increase (0.5 units) after passing a slight decline at around 20 min of precipitation time.

These findings are in good agreement with the results from studies on the binary Cu/Zn systems carried out by Schlögl et al. [7]. These authors varied the composition of Cu/Zn precursors obtained at pH 7 and observed a pH drop after ca. 20 min for precipitates with a high Cu/Zn ratio. Furthermore, according to results of Kiener et al. [18], who studied the binary Cu/Zn system on a broader time scale of aging, all samples obtained at pH >6 exhibited a slow, constant rise of pH within hours, reaching a plateau at pH 8. These authors suggested that this phenomenon may be linked to the continuous incorporation of carbon dioxide into the solid during stirring in form of carbonate while releasing the hydroxide.

Cat_2 (see Fig. 6), one of the most active catalysts in the methanol productivity screening, was chosen for a more detailed study of the influence of controlled or uncontrolled precursor aging on later catalytic activity. To study the origin of the sudden pH increase after 20–25 min of aging specimens were isolated after different time periods during the controlled and uncontrolled aging process at 70 °C and an initial pH of 7. The results are shown in Fig. 14.

The specimens taken at 10 (a) and 20 (b) min did not show any evidence for crystalline phases (Fig. 15). After 20 min, crystallization of the hydroxy carbonate phase (presumably malachite or Cu/Zn malachite) coincided with the change in pH, indicating transformation of the solid. A similar crystallization phenomenon occurring after this approximate time period was reported for the binary system by Bems et al. [7] and Muhamad et al. [33]; however, in those cases, rosasite and aurichalcite were observed at a

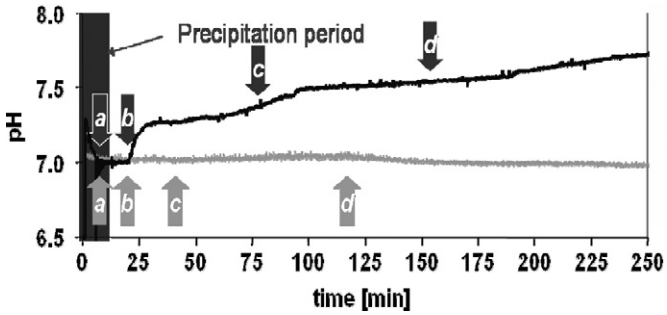

Fig. 14. pH evolution of the Cat_2 precursor precipitated at pH 7 (70 °C); dark curve: free-aging process, grey curve: controlled aging process at pH 7_{const}. Arrows indicate when samples were taken.

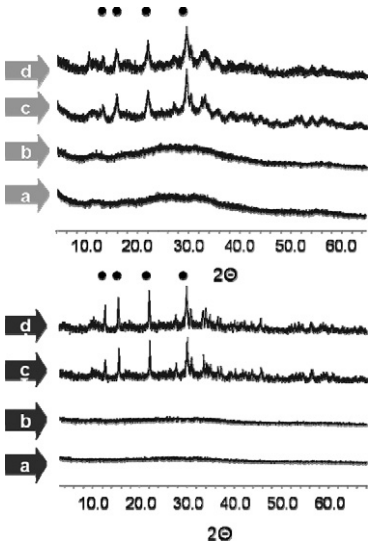

Fig. 15. XRD measurements of precursor samples taken during the aging process: (●) Cu/Zn malachite; colors and letters correspond to marked samples in Fig. 14.

Cu/Zn ratio of 70/30. We observed this same development for both the free-aged and pH-controlled precursors. The pH-controlled catalyst precursor samples (c) and (d), obtained at 90 and 180 min (Fig. 14, gray line) had the characteristic XRD pattern of malachite species (Fig. 15). The free-aged precipitate samples (c) and (d) (Fig. 14, dark line), obtained at 50 and 150 min, also consisted of malachite species. XRD analysis revealed no reflection shifts or reflection shape alterations for this malachite phase after the longer aging time, indicating termination of crystal growth; thus, we conclude that a stable state must have been achieved.

In addition, we observed broader malachite or zincian malachite reflection peaks for the controlled-aged catalyst precursors compared with the free-aged samples. This finding indicates the formation of comparatively smaller particles of this characteristic phase.

Most of the precursors obtained at temperatures below 70 °C and at slightly acidic, neutral, or basic pH exhibited characteristic XRD patterns of a zinc aluminum nitrate hydroxide ($Zn_2Al(OH)_6NO_3{\cdot}1.9H_2O$), which could not be specified in more detail, and copper nitrate hydroxide (rouaite, $Cu_2(NO_3)(OH)_3$). The well-defined shape and high intensity of the presumed aluminum nitrate hydroxide phase reflections suggest the formation of relatively large particles. A typical XRD pattern of precursors obtained at low pH is shown in Fig. 16.

Most of the precursor phases obtained under alkaline conditions and temperatures above 50 °C contained poorly crystallized zinc–aluminum-nitrate-hydroxide or were completely XRD amorphous. The nitrate-hydroxide reflections were more pronounced

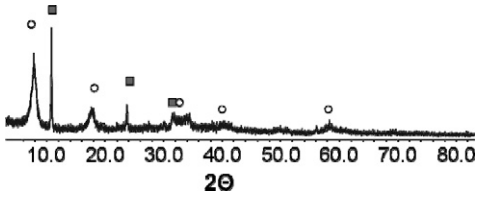

Fig. 16. XRD pattern of a typical precursor sample obtained at low pH values: (○) rouaite, $Cu_2(NO_3)(OH)_3$; (■) zinc aluminum nitrate hydroxide, $Zn_2Al(OH)_6NO_3{\cdot}1.9H_2O$.

in the precipitates obtained at low pH. The characteristic diffraction peaks of zinc–aluminum-nitrate-hydroxides or rouaite were not seen in the calcined samples (Fig. 7). These phases presumably were decomposed during the calcination process. In comparison, the malachite phase formation observed during the aging process was shown as nondecomposed residue in the calcined catalysts (Fig. 7).

The important role of pH in determining the phase composition of the precipitates has been reported by many authors. Li et al. [20] and Wasserman et al. [34] proposed the following reaction model, which can be applied and modified for the catalytic systems investigated here:

$$Cu^{2+} + 2OH^- \rightarrow Cu(OH)_2(s),$$
$$3Cu(OH)_2(s) + Cu^{2+} + 2NO_3^- \rightarrow Cu(NO_3)_2{\cdot}3Cu(OH)_2(s),$$
$$Cu(OH)_2(s) + Cu^{2+} + CO_3^{2-} \rightarrow Cu_2(OH)_2CO_3(s),$$
$$Cu(OH)_2(s) + Zn^{2+} + CO_3^{2-} \rightarrow (Cu,Zn)_2(OH)_2CO_3.$$

Along with the decrease in pH, the concentration of H^+ ions increases, leading to a decrease in carbonate concentration due to the shift of the equilibrium,

$$H^+ + CO_3^{2-} \rightleftharpoons HCO_3^-,$$

toward the right side. This suppresses the formation of malachite and other hydroxy carbonates, giving rise to the formation of nitrate phases at low pH. Those earlier studies also revealed a typical malachite-type phase in some of the catalysts, giving high methanol synthesis activity.

These findings are in good agreement with the findings of Klier [35] indicating that during calcination, ZnO can be formed in different morphologies (hexagonal or prismatic). Hydroxy nitrates as the dominant phase might act as a seed for crystallization of the nascent zinc oxide, favoring the formation of hexagonal platelets at the expense of prismatic structures. The platelets should provide a larger surface area and thus higher activity; therefore, high amounts of nitrate phases with precursors with large particle sizes may indicate low productivity in the catalyst created from such a precursor. Furthermore, it is reasonable to suppose that the interdispersion of CuO and ZnO is more intimate after calcination of mixed hydroxy carbonate precursors, in which both metals are in close conjunction [20].

The beneficial effect of higher temperature may be explained by the fact that the precipitation proceeds under less oversaturated conditions and hence at a lower rate. As a result, a more uniform precipitate is generated, containing homogeneously distributed copper and zinc species.

The affect of precipitate aging time on catalytic performance was investigated by comparing another batch of precursors of the Cu/Zn/Al catalysts Cat_2 and Cat_3 and a binary catalyst precursor composed only of the nitrate solutions of Cu and Zn at pH 7 and 70 °C to study the affect of aluminum on catalyst performance. The Cu/Zn molar ratio for this catalyst was set to be 70/30, which corresponds to the composition used by Bems et al., who previously investigated the aging behavior of the binary system but did not perform catalytic tests on these samples [7]. The precursor of

Table 1
Binary and ternary catalysts prepared under different aging conditions

Catalyst	Metals (molar ratio)	Precipitation parameters	Aging parameters
$Cat_{2\text{-const}}$	Cu/Zn/Al (60/30/10)	pH 7, 70 °C	pH 7_{const}, 70 °C
Cat_3	Cu/Zn/Al (60/30/10)	pH 8, 70 °C	pH 8_{const}, 70 °C
$Cat_{2\text{-free}}$	Cu/Zn/Al (60/30/10)	pH 7, 70 °C	Free-aged, 70 °C
$Cat_{Cu/Zn}$	Cu/Zn (70/30)	pH 7, 70 °C	pH 7_{const}, 70 °C

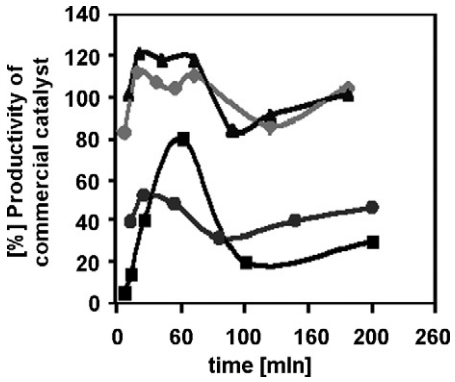

Fig. 17. Methanol productivity as a function of the aging time for selected catalysts: (▲) $Cat_{2\text{-const}}$; (■) $Cat_{2\text{-free}}$; (●) $Cat_{Cu/Zn}$; (◆) Cat_3.

Cat_2 (pH 7, 70 °C) was again resynthesized but aged without pH control. During the aging process of the binary precursor and the three different ternary precursors, samples of the suspension were obtained, filtered, washed, dried, and calcined under standard conditions (300 °C, 4 h). The preparation conditions for the binary and ternary catalysts are summarized in Table 1. The methanol synthesis activity of all catalysts was evaluated in the high-throughput setup under the same reaction conditions. Fig. 17 illustrates the results. All of the catalysts obtained from the precursor samples exhibited the same aging time-dependent characteristics. At short aging times, activity was low. It increased up to aging times of 20–50 min, depending on the system. After about 1 h of aging time, the activity dropped again, and subsequently increased slightly for longer aging times.

These findings apply for all four catalysts investigated. The ternary Cu/Zn/Al catalysts achieved the highest activity when aged under controlled conditions, with $Cat_{2\text{-const}}$ giving the highest methanol productivity (ca. 130% of the productivity of the commercial catalyst). Samples of Cat_3 (pH 8, 70 °C) exhibited similar behavior at all aging times, with slightly lower activity than that of $Cat_{2\text{-const}}$. A more pronounced affect of aging time on catalytic performance was observed for the catalyst aged without pH control ($Cat_{2\text{-free}}$): At the start of the aging process, almost no methanol synthesis activity was observed. The activity rose rapidly with increasing aging time, passing a sharply pronounced culmination point at 60 min. The maximum productivity was 40% lower than that for the pH-controlled samples of Cat_2. Subsequently the activity dropped again, then recovered slowly with increasing aging time.

The binary catalyst achieved only around 50% of the catalytic activity of the ternary Cu/Zn/Al system while exhibiting a similar methanol productivity-aging curve as the other catalysts studied (Fig. 17). A more pronounced aging effect for the binary system on the activity of the final catalyst was reported by Waller et al. for a Cu/Zn 2:1 catalyst [32], with a greater initial increase in a nonaged precursor than in a precursor aged for 30 min. But in the system that those authors studied, the initial nonaged precursor was already crystalline, whereas in the study of Bems et al. [7], amorphous precursors were obtained for the initial samples. This may be related to the fact that Waller et al. used separate precipitation and aging vessels, and thus their unaged samples also had been exposed to the mother liquor for some time in the precipitation vessel. For the binary system, Ressler et al. [30] found TEM evidence indicating that the pronounced activity increase on crystallization of the precursor during aging was due to a more intimate interaction of Cu and ZnO in the final catalyst. They also found such a correlation for Cu/ZnO catalysts used in methanol steam reforming. Activity was increased for aged crystalline precursors, and the copper microstrain resulting from the intimate contact between Cu and ZnO led to higher catalytic activity [36].

The lower activity of all free-aged samples of Cat_2 (Fig. 6) compared with the pH-controlled samples may be due to the formation of larger hydroxy carbonate crystallites after 20 min of aging (Fig. 15), resulting in large Cu/Zn oxide particles after calcination. Decreased catalytic activity was observed at 60–100 min, but the characteristic hydroxy carbonate diffraction pattern remained, as shown in Fig. 15.

Comparing $Cat_{2\text{-const}}$ and the binary Cu/Zn catalyst with the same Cu/Zn metal ratio clearly shows the significant promoter role of Al (Fig. 17). It is known that Al^{3+} can help form zinc aluminate, which prevents the agglomeration of Cu particles and stabilizes the highly dispersed Cu/ZnO crystallites. At the same time, it also facilitates and accelerates the adsorption of CO due to its structural disorder and defect surface domains [37]. Chen et al. [38] reported that M^{3+} ions can enhance the formation of monovalent cationic defects on the crystal surface of ZnO, accelerating both the enrichment and stabilization of Cu^+ on the surface during the reduction and reaction processes. In addition, the formation of a $CuAl_2O_4$ surface spinel phase with a different reduction behavior has been proposed as a cause of the promoter effect of aluminum [1,39]. This also may contribute to the enhanced activity of aluminum-containing samples.

4. Conclusion

In this study, we systematically prepared ternary $Cu/ZnO/Al_2O_3$ catalysts via a coprecipitation route under strictly controlled pH, precipitation temperature, and calcination temperature. We evaluated the catalysts' methanol synthesis activity in a 49-channel parallel reactor under reaction conditions similar to those of the commercial methanol production route. Detailed correlations between synthesis conditions, catalyst structure and texture, and catalytic performance were established. The greatest methanol productivity was found for catalysts with the following "preparation history": precipitation temperature of 70 °C, pH of 6–8, aging time of 20–60 min, and calcination at 300 °C. In general, the high productivity of the catalysts obtained under these conditions was correlated with relatively high BET and Cu(0) surface areas in the same range.

The most active catalysts were seen to contain malachite-type residues from the initial hydroxy carbonate precipitate in the calcined precursor. The presence of hydroxy carbonate phases after calcination greatly enhanced the catalytic properties of the final $Cu/ZnO/Al_2O_3$ catalysts. Residual hydroxy carbonates presumably facilitated the formation of highly active sites during reduction, as is known from previous studies on binary Cu/Zn hydroxy carbonates [10]. The Cu/Zn malachite residues in the calcined catalyst favored the formation of CuO crystallites and Cu^0 nanoparticles during catalyst reduction. The particles obtained were smaller than the particles derived from pure Cu phases, such as CuO, which were found predominantly at low pH during precursor synthesis. Both the CuO/ZnO and then the reduced Cu/ZnO phase were derived from Zn/Cu malachite. With its isomorphous structure of Cu and Zn species, which can easily exchange their positions, Zn/Cu malachite allowed both metals to undergo greater interaction than can occur in pure phases [28]. The presence of carbonate residues presumably delayed the fragmentation of the catalyst structure be-

fore the reduction of the copper species begins. As a result, smaller, more interactive particles were formed. This was confirmed by TEM investigations, with the micrographs revealing that 10-nm copper particles were closely connected to the ZnO matrix. The residual hydroxy carbonates in the calcined precursor may have facilitated the catalyst activation procedure, allowing a much "gentler" reduction process.

The hydroxy carbonate precursor most likely was partially decomposed during the catalyst reduction period. The productivities measured for the samples reduced without calcination were close to those measured for catalysts that had been calcined at 200 or 300 °C. Calcination temperatures above 300 °C resulted in the formation of pure CuO phases. The catalysts obtained after calcination at these temperatures showed decreasing methanol synthesis activity.

We also have confirmed that the postprecipitation history of the precursor material can strongly influence the catalyst activity. Comparison of precursors aged with and without pH control revealed that the essential phase formation, especially that of the hydroxy carbonates, occurred after ca. 20 min, coinciding with a rapid pH increase in the free-aged samples. The greatest catalytic activities were achieved for catalysts aged for 20–60 min, indicating that the first 20 min are crucial for copper and zinc phase formation.

Acknowledgments

Funding in addition to the basic support by the Max Planck Society was provided by the DFG (SFB 558). The authors thank Mr. B. Spliethoff for the TEM measurements and Dr. C. Weidenthaler for the *in situ* XRD measurements. They also thank ICI Synetix for providing the industrial benchmark catalyst.

References

[1] R.T. Figueiredo, A. Martinez-Arias, M. Lopez Granados, J.L.G. Fierro, J. Catal. 178 (1998) 146.
[2] G.C. Chinchen, K. Mansfield, M.S. Spencer, Chemtech (1990) 693.
[3] R.G. Herman, Stud. Surf. Sci. Catal. 27 (1991) 266.
[4] K.C. Waugh, Catal. Today 15 (1992) 51.
[5] P.B. Rasmussen, M. Kazuta, Y. Chorkendorff, Surf. Sci. 318 (1995) 313.
[6] R.G. Herman, K. Klier, G.W. Simmons, P.B. Finn, J.B. Bulko, T.P. Kobylinsky, J. Catal. 56 (1979) 407.
[7] B. Bems, M. Schur, A. Dassenoy, H. Junkes, D. Herein, R. Schlögl, Chem. Eur. J. 9 (2003) 2039.
[8] B.L. Kniep, T. Ressler, A. Rabis, F. Girgsdies, M. Baenitz, F. Steglich, R. Schlögl, Angew. Chem. Int. Ed. 43 (2004) 112.
[9] M.M. Günther, T. Ressler, B. Bems, C. Büscher, T. Genger, O. Hinrichsen, M. Muhler, R. Schlögl, Catal. Lett. 71 (2001) 37.
[10] J.C.J. Bart, R.P.A. Sneeden, Catal. Today 2 (1987) 122.
[11] G.C. Chinchen, P.J. Denny, J.R. Jennings, M.S. Spencer, K.C. Waugh, Appl. Catal. 36 (1988) 1.
[12] L.M. Plyasova, T.M. Yur'eva, T.A. Kriger, O.V. Makarova, V.I. Zaikovskii, L.P. Soloveva, A.N. Shmakov, Kinet. Catal. 36 (1995) 425.
[13] G.J. Millar, I.H. Holm, P.J. Uwins, J. Drennan, J. Chem. Soc. Faraday Trans. 94 (1998) 593.
[14] G.-C. Shen, S.-I. Fujita, S. Matsumuto, N. Takezawa, J. Mol. Catal. A 124 (1997) 123.
[15] B. Jandeleit, D.J. Schaefer, T.S. Powers, H.W. Turner, W.H. Weinberg, Angew. Chem. Int. Ed. 38 (1999) 2494.
[16] S. Senkan, Angew. Chem. Int. Ed. 40 (2001) 312.
[17] M.T. Reetz, Angew. Chem. Int. Ed. 40 (2001) 284.
[18] C. Kiener, M. Kurtz, H. Wilmer, C. Hoffmann, H.-W. Schmidt, J.-D. Grunwaldt, M. Muhler, F. Schüth, J. Catal. 216 (2003) 110.
[19] S. Olejnik, C. Baltes, M. Muhler, F. Schüth, J. Comb. Chem. 10 (2008) 287.
[20] J.-L. Li, T. Inui, Appl. Catal. A Gen. 137 (1996) 105.
[21] J. Skrzypek, J. Sloczynski, S. Ledakowicz, Methanol Synthesis—Science and Engineering, Polish Scientific Publisher, Warszawa, 1994.
[22] J.B. Hansen, P.E.J. Nielsen, in: G. Ertl, H. Knözinger, F. Schüth, J. Weitkamp (Eds.), Handbook of Heterogeneous Catalysis, second ed., Wiley–VCH, Weinheim, 2008, p. 2920.
[23] W.X. Pan, R. Cao, D.L. Roberts, G.L. Griffin, J. Catal. 114 (1988) 440.
[24] J.F. Deng, Q. Sun, Y.L. Shang, S.Y. Chen, D.A. Wu, Appl. Catal. A Gen. 139 (1996) 75.
[25] G.C. Chinchen, K.C. Waugh, D.A. Whan, Appl. Catal. 25 (1986) 101.
[26] R. Becker, H. Parala, F. Hipler, O.P. Tkachenko, K.V. Klementiev, W. Grünert, H. Wilmer, O. Hinrichsen, M. Muhler, A. Birkner, C. Wöll, S. Schäfer, R.A. Fischer, Angew. Chem. Int. Ed. 43 (2004) 2839.
[27] M. Schur, B. Bems, A. Dassenoy, I. Kassatikine, J. Urban, H. Wilmers, O. Hinrichsen, M. Muhler, R. Schlögl, Angew. Chem. Int. Ed. Engl. 42 (2003) 3815.
[28] I. Melian-Cabrera, M. Lopez Granados, J.L.G. Fierro, Catal. Lett. 84 (2002) 153.
[29] D.M. Whittle, A.M. Mirzaei, J.S.J. Hargreaves, R.W.J.C. Kiely, S.H. Taylor, G. Hutchings, Phys. Chem. Chem. Phys. 4 (2002) 5915.
[30] T. Ressler, B.L. Kniep, I. Kasatkin, R. Schlögl, Angew. Chem. Int. Ed. 44 (2005) 4704.
[31] L.M. Plyasova, T.M. Yur'eva, T.A. Kriger, O.V. Makarova, V.I. Zaikovskii, L.P. Solov'eva, A.N. Shmakov, Kinet. Catal. 36 (1995) 425.
[32] D. Waller, D. Stirling, F.S. Stone, M.S. Spencer, Faraday Discuss. 87 (1989) 107; S.H. Taylor, G.J. Hutchings, A.A. Mirzaei, Chem. Commun. (1999) 1373.
[33] E.N. Muhamad, R. Irmawati, Y.H. Taufiq-Yap, A.H. Abdullah, B.L. Kniep, F. Girgsdies, T. Ressler, Catal. Today 131 (2008) 118.
[34] I.M. Wasserman, N.I. Silanteva, Russ. J. Inorg. Chem. 13 (1968) 1041.
[35] K. Klier, Adv. Catal. 32 (1982) 243.
[36] B.L. Kniep, F. Girgsdies, T. Ressler, J. Catal. 236 (2005) 34.
[37] X. Liu, G.Q. Lu, Z. Yan, J. Beltramini, Ind. Eng. Chem. Res. 42 (2003) 6518.
[38] H. Chen, D. Liao, L. Yu, Y. Lin, H. Zhang, K. Tsai, Appl. Surf. Sci. 147 (1999) 85.
[39] P. Porta, S. Morpurgo, I. Pettit, J. Solid State Chem. 121 (1996) 372.